Variable-range hopping conductivity in La_{1-x} Ca_x Mn_{1-y} Fe_y O_3: evidence of a complex gap in density of states near the Fermi level

2002 J. Phys.: Condens. Matter 14 8043

(http://iopscience.iop.org/0953-8984/14/34/323)

INSTITUTE OF PHYSICS PUBLISHING JOURNAL OF PHYSICS: CONDENSED MATTER

J. Phys.: Condens. Matter **14** (2002) 8043–8055 PII: S0953-8984(02)36797-3

Variable-range hopping conductivity in $La_{1-x}Ca_xMn_{1-y}Fe_yO_3$: evidence of a complex gap in density of states near the Fermi level

R Laiho[1], K G Lisunov[1,2], E Lähderanta[1,3], P A Petrenko[2], J Salminen[1], M A Shakhov[1,4], M O Safontchik[1,4], V S Stamov[1,2], M V Shubnikov[1,4] and V S Zakhvalinskii[1,2]

[1] Wihuri Physical Laboratory, Department of Physics, University of Turku, FIN-20014 Turku, Finland
[2] Institute of Applied Physics, Academiei Str. 5, MD-2028 Kishinev, Moldova
[3] Physics, University of Vaasa, PO Box 700, FIN-65101 Vaasa, Finland
[4] A F Ioffe Physico-Technical Institute, 194021, St Petersburg, Russia

Received 9 May 2002
Published 15 August 2002
Online at stacks.iop.org/JPhysCM/14/8043

Abstract

The resistivity, ρ, of ceramic $La_{1-x}Ca_xMn_{1-y}Fe_yO_3$ with $x = 0.3$ and $y = 0.0$–0.09 is found to obey, between a temperature $T_v \approx 310$–330 K and the ferromagnetic-to-paramagnetic transition temperature, $T_C = 259$–119 K (decreasing with y), the Shklovskii–Efros-type variable-range hopping conductivity law, $\rho(T) = \rho_0(T)\exp[(T_0/T)^{1/2}]$. This behaviour is governed by generation of a soft Coulomb gap $\Delta \approx 0.42$ eV in the density of localized states and a rigid gap $\delta(T) \approx \delta(T_v)(T/T_v)^{1/2}$ with $\delta(T_v) \approx 0.16$, 0.13 and 0.12 eV at $y = 0.03$, 0.07 and 0.09, respectively. Deviations from the square root dependence of $\delta(T)$, decreasing when y is increased, are observed as $T \to T_C$. The prefactor of the resistivity follows the law $\rho_0(T) \sim T^m$, where m changes from $9/2$ at $y = 0$ to $5/2$ in the investigated samples with $y = 0.03$, 0.07 and 0.09, which is connected to introduction of an additional fluctuating short-range potential by doping with Fe.

(Some figures in this article are in colour only in the electronic version)

1. Introduction

The colossal magnetoresistance (CMR) or huge drop in the resistivity ρ in an external magnetic field, B, near the paramagnetic (PM) to ferromagnetic (FM) transition temperature, T_C, of $La_{1-x}Ca_xMnO_3$ (LCMO) and related mixed-valence manganites, has attracted much interest since its discovery [1, 2]. In addition to Mn^{3+}, these compounds contain Mn^{4+} as a result of substitution of a divalent alkaline element for La^{3+} (hole doping). It is generally believed that the conductivity of manganites is governed above T_C by hopping of small polarons connected

to local Jahn–Teller distortions [3] and that the large drop in $\rho(T)$ near the resistivity maximum, T_m, which is close to T_C, in compounds with $x \approx 0.33$ is due to a metal–insulator transition [4]. In particular, the adiabatic nearest-neighbour hopping (NNH) of small polarons leading to $\rho(T) = \rho_0 \exp(W_h/kT)$, with $\rho_0 \sim T$ and $W_h = 865$ K, has been observed in bulk and film LCMO samples within a wide interval of $T = 300$–700 K [5].

Below room temperature down to T_C both the NNH polaron model [6, 7] and the Mott variable-range hopping (VRH) conductivity mechanism [8–10] were applied to interpret the resistivity of different mixed-valence manganites. The point is that, in disordered materials, the probability of finding an empty nearest site with a proper energy level decreases rapidly with lowering temperature. Therefore, the conductivity is determined by competition of two processes, connected to hopping between the nearest sites with large energy differences or to hopping between sites beyond the nearest neighbours with small energy differences. Mott [11] was the first to show that, under these conditions, hopping is possible inside an optimum energy strip $(\varepsilon_{max} - \mu, \varepsilon_{max} + \mu)$ around the Fermi level, μ. For constant density of the localized states (DOS) inside the interval of $(\varepsilon_{max} - \mu, \varepsilon_{max} + \mu)$ he found the law $\rho(T) = \rho_0 \exp[(T_{0M}/T)^{1/4}]$. In general, transition to the VRH conductivity with lowering T, supposed in [8–10], is physically plausible due to the universality of Mott's conclusion about the role of the optimum energy strip in hopping conductivity. However, the results of these works need some reconsideration from the viewpoint that the behaviour of the DOS inside the interval $(\varepsilon_{max} - \mu, \varepsilon_{max} + \mu)$ is non-universal.

Shklovskii and Efros (SE) [12] have shown that, due to the Coulomb interaction between the localized charge carriers, a soft parabolic gap, Δ, appears in the DOS in the interval of $(\mu - \Delta, \mu + \Delta)$, giving rise to the resistivity $\rho(T) = \rho_0 \exp[(T_{0SE}/T)^{1/2}]$. Therefore, the effects connected to the Coulomb gap may be neglected until the relation of $\varepsilon_{max}(T) > \Delta$ is satisfied. This may be possible if the temperature is sufficiently high or the Coulomb interaction between the carriers is small. In LCMO with $x \approx 0.33$ the average distance between the holes is about the lattice parameter, resulting in a strong Coulomb interaction. Therefore, neglect of Δ when lowering the temperature requires special substantiation.

It appears that in manganites the behaviour of DOS is even more complicated. In the scanning–tunnelling spectroscopy study of a LCMO film with $x = 0.2$ parabolic dependence of DOS on energy, $g(\varepsilon)$, was found inside an interval of $\sim$0.4 eV around μ at T between $\sim$160 and 370 K [13]. In addition, for T near $T_m = 196$ K a rigid gap ($g(\varepsilon) = 0$) with width $\delta \approx 0.11$ eV around μ was observed. This gap has a maximum at T shifted from T_C and vanishes below $\sim$155 K. The soft gap was attributed to Coulomb interactions between localized electrons and the rigid gap to the Jahn–Teller effect [13].

Another detail, which has not received sufficient attention in the analysis of the resistivity of manganites, is the temperature dependence of the prefactor ρ_0. The point is that both the Mott and SE models were proposed initially to interpret the VRH conductivity usually found in doped crystalline semiconductors at liquid helium temperatures with negligible dependence of ρ_0 on T. Because in LCMO and the related CMR materials the hopping conductivity is observed at much higher temperatures, extrapolation of $\rho_0(T)$ from the low-temperature region is not justified.

Due to the similarity of the ionic radii of Mn^{3+} and Fe^{3+}, doping with iron is expected to cause only minor lattice distortions in $La_{1-x}Ca_xMn_{1-y}Fe_yO_3$ (LCMFO) [14]. At a low doping level direct replacement of Mn^{3+} by Fe^{3+} is expected [15], introducing additional antiferromagnetic interactions [16]. This is one of the reasons leading to a considerable diminution of T_C in LCMFO when y is increased [14]. Another reason is the additional microscopic disorder in the cation sublattice introduced by doping with Fe [17]. The strong dependence of T_C on y offers a good possibility for investigations of the VRH conductivity in LCMFO.

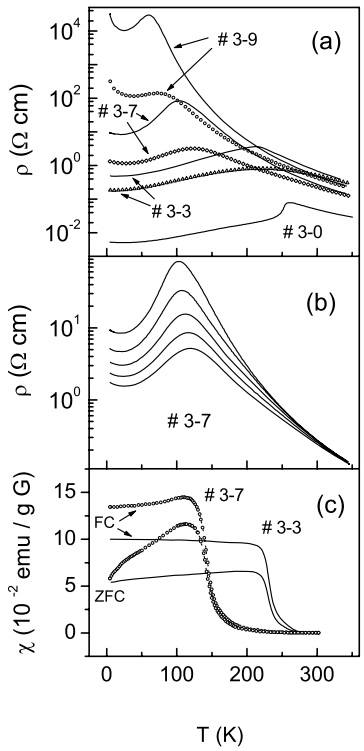

Figure 1. (a) Temperature dependence of the resistivity of the investigated samples in zero field (full curves) and in the field of 10 T (open symbols). (b) Temperature dependence of the resistivity of no 3-7 measured in the field of $B = 0, 2, 4, 6$ and 8 T (from top to bottom). (c) Temperature dependence of χ_{ZFC} and χ_{FC} measured in the field of $B = 2$ G for no 3-3 (full curves) and for no 3-7 (open symbols).

In this paper we investigate the temperature dependence of the resistivity of LCMFO, paying special attention to the electronic spectrum and the conductivity mechanism. Such investigations are expected to provide important microscopic information about localized charge carriers in this compound.

2. Experimental results

LCMFO with $x = 0.3$ and $y = 0$, 0.03, 0.07 and 0.09 (samples no 3-0, 3-3, 3-7 and 3-9, respectively) were synthesized with standard ceramic procedures by heating stoichiometric mixtures of La_2O_3, $CaCO_3$, Mn_2O_3 and Fe_2O_3 in air at 1320 °C, at first for 15 h and then for 5 and 15 h and finally at 1375 °C for 22 h, with intermittent grindings. According to x-ray diffraction data the iron-doped samples have the same undistorted cubic structure (space group *Pm3m*) as undoped $La_{0.7}Ca_{0.3}MnO_3$ (sample no 3-0) [18]. Investigations of $\rho(T)$ were made using the conventional four-probe technique in the transverse magnetic field configuration ($\boldsymbol{B} \perp \boldsymbol{j}$) for $B = 0$–10 T. The sample probe was inserted in a He exchange gas dewar, where its temperature could be varied between 4.2 and 350 K to an accuracy of 0.5%. Magnetization $M(T)$ was measured with an rf-SQUID magnetometer after cooling the sample from room temperature down to 5 K in zero dc field (ZFC) or in the field of $B = 2$ G (FC). The temperature of the sample space was controlled to an accuracy of ± 1 K.

The plots of $\rho(T)$ shown in figure 1(a) for no 3-0, 3-3, 3-7 and 3-9 for $B = 0$ (full curves) and 10 T (open symbols) and in figure 1(b) for no 3-7 and B between 0–10 T, are

Table 1. The values of the relative concentrations of Fe y, the PM–FM transition temperature T_C, the temperature of the onset of VRH T_v, the characteristic VRH temperatures T_0, the coefficients A, the width of the Coulomb gap Δ, the ratio b_1/b_2, the width of the rigid gap $\delta(T_v)$ and the localization radius a.

Sample no	y	T_C (K)	T_v (K)	T_0 (10^4 K)	A (Ω cm K^{-m})	Δ (eV)	b_1/b_2	$\delta(T_v)$ (eV)	a (Å)
3-0	0.01	259	319	8.1	2.5×10^{-20}	0.44	—	—	—
3-3	0.03	228	≈330	7.7	5.0×10^{-14}	0.43	1.31 ± 0.05	0.16	2.9
3-7	0.07	139	310	7.3	3.0×10^{-14}	0.40	1.26 ± 0.06	0.13	2.7
3-9	0.09	119	316	7.7	3.5×10^{-14}	0.41	1.21 ± 0.04	0.12	2.5

typical for hole-doped manganite perovskites, including with decreasing T a strong increase up to a maximum at T_m, a decrease with lowering T further and a weak dependence in the low-temperature region. Both ρ and the drop of $\rho(T)$ near T_m between $B = 0$ and 10 T are increased strongly when y is increased. Additionally, in no 3-9 $\rho(T)$ starts to increase again with lowering T sufficiently below T_m. Generally, the observed dependence of ρ on T, B and y agrees with the behaviour known from literature [9, 14].

The plots of $\chi_{ZFC}(T)$ and $\chi_{FC}(T)$ (where $\chi = M/B$) for sample no 3-0 are similar to those in figure 1(c) for no 3-3 and in the case of no 3-9 to those in figure 1(b) for no 3-7. All the samples exhibit a steep PM–FM transition with T_C decreasing strongly when y is increased (see table 1). Magnetic irreversibility (deviation of $\chi_{ZFC}(T)$ from $\chi_{FC}(T)$) is observed just below the transition.

3. Discussion

Following the discussion in the introduction, the resistivity can be written in a universal form:

$$\rho(T) = \rho_0(T) \exp[(T_{0j}/T)^p], \tag{1}$$

where the prefactor $\rho_0(T)$ and the characteristic temperature T_{0j} depend on the hopping mechanism. Hopping over the nearest sites (NNH) corresponds to the value of $p = 1$, while the VRH conductivity governed by the Mott and SE mechanisms is characterized by $p = 1/4$, $T_{0j} = T_{0M}$ or $p = 1/2$, $T_{0j} = T_{0SE}$, respectively, where

$$T_{0M} = \beta_M/[kg(\mu)a^3] \qquad \text{and} \qquad T_{0SE} = \beta_{SE}e^2/(\kappa ka). \tag{2}$$

Here $\beta_M = 21$, $\beta_{SE} = 2.8$ and $g(\mu)$ is the DOS at the Fermi level, a is the localization radius of charge carriers and κ is the dielectric constant [11, 12].

In conventional doped semiconductors when both T and T_{0j} are small the strong inequality (see appendix)

$$\Gamma \equiv \left[\frac{kT(T_{0j}/T)^p a}{2\hbar s}\right]^2 \ll 1 \tag{3}$$

is satisfied and the temperature dependence of $\rho_0(T)$ is weak [19] (see table 2). For the mixed-valence manganites $T_{0M} \sim 10^3$–10^6 and $a \sim$ 1–9 Å have been reported [8–10]. Together with observations of VRH up to room temperature, these data contradict the inequality (3) (for estimations one can use $s = 6.8 \times 10^5$ cm s^{-1} for LCMO [20]), but are consistent with $\Gamma \gg 1$. An analysis of the resistivity of the CMR compounds without taking into account this difference may contain a source of error.

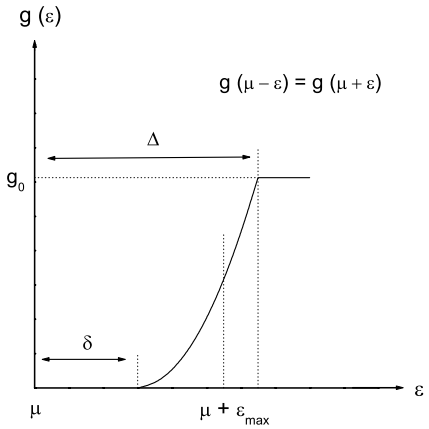

Figure 2. Density of states near the Fermi level μ at the energy $\varepsilon > \mu$. Δ is the width of the soft Coulomb gap, δ is the width of the rigid gap and ε_{max} is the width of the optimum energy strip.

Table 2. Values of p and m for different regimes of VRH.

The type of VRH and wavefunction	q	p	m ($\Gamma \ll 1$)	m ($\Gamma \gg 1$)
SE, $\psi(r) \sim \exp(-r/a)$	0	1/2	1/2	9/2
Mott, $\psi(r) \sim \exp(-r/a)$	0	1/4	1/4	25/4
SE, $\psi(r) \sim r^{-1}\exp(-r/a)$	4	1/2	−3/2	5/2
Mott, $\psi(r) \sim r^{-1}\exp(-r/a)$	4	1/4	−3/4	21/4

Another important point is the possible existence of the rigid gap around the Fermi level. The DOS, containing both the soft parabolic Coulomb gap Δ and the rigid gap δ, is given by $g(\varepsilon) = 0$ for $\mu - \delta < \varepsilon < \mu + \delta$, $\alpha_3(\kappa^3/e^6)(\varepsilon - \mu + \delta)^2$ for $\mu - \Delta < \varepsilon < \mu - \delta$, $\alpha_3(\kappa^3/e^6)(\varepsilon - \mu - \delta)^2$ for $\mu + \delta < \varepsilon < \mu + \Delta$ and g_0 for $\varepsilon < \mu - \Delta$ and $\varepsilon > \mu + \Delta$, where g_0 is the value of the DOS outside the gap and $\alpha_3 = 3/\pi$ [12]. $g(\varepsilon)$ is symmetric around the Fermi level (see figure 2 for $\varepsilon > \mu$) and coincides at $\delta = 0$ with the DOS that contains only the Coulomb gap [12].

The expressions for the prefactor ρ_0 and the characteristic temperature T_0 for the case of DOS given above (figure 2) and for an arbitrary value of Γ are obtained in the appendix. In the limiting cases of $\Gamma \ll 1$ and $\Gamma \gg 1\rho_0(T)$ is given by the equation

$$\rho_0(T) = AT^m, \tag{4}$$

where A is a constant (see the appendix) and the values of m are collected in table 2. It can be seen that the temperature dependence of ρ_0 is quite different for $\Gamma \ll 1$ and $\Gamma \gg 1$. Additionally, the form of the localized carrier wavefunction, depending on the presence or absence of a fluctuating short-range potential, is important (this is given by the value of q—see the appendix). The characteristic temperature satisfies the equation

$$T_0 = \left(\frac{\delta}{2k\sqrt{T}} + \sqrt{\frac{\delta^2}{4k^2T} + T_{0SE}}\right)^2. \tag{5}$$

In the cases when T_0, given by equation (5), is independent of T, equation (1) (with $T_{0j} = T_0$), (4) and (5) give the temperature dependence of the resistivity directly. If a is independent of T, these cases are (i) $\delta = 0$, (ii) $\delta/(2kT) \ll (T_{0SE}/T)^{1/2}$ and $\delta \sim T$ and (iii) $\delta \sim T^{1/2}$. For (i) and (ii) we find that $T_0 = T_{0SE}$ (in case (ii) $\xi_c \approx (T_{0SE}/T)^{1/2} + \delta/(2kT)$, and if $\delta \sim T$, the second term is constant and can be included in the prefactor), while in the third case $T_0 \neq T_{0SE}$.

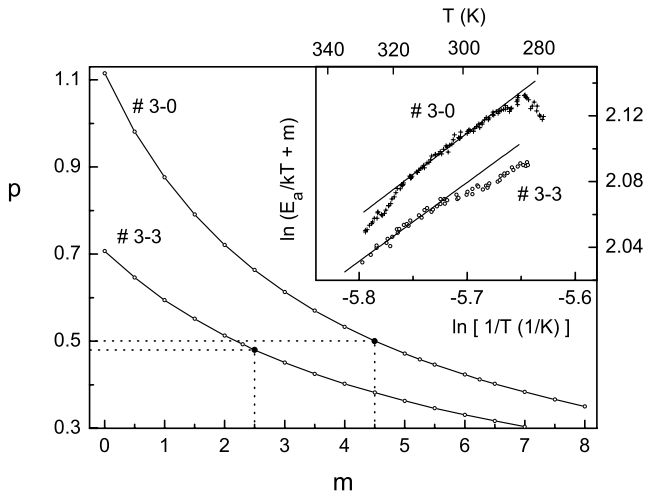

Figure 3. Dependence of p on m for no 3-0 and no 3-3. Inset: dependence of $\ln(E_a/kT + m)$ on $\ln(1/T)$ for $m = 9/2$ (no 3-0) and $5/2$ (no 3-3). The lines are fits to the experimental data.

Taking into account the data from table 2 for VRH conductivity at different limits of Γ we have, together with the NNH conductivity (where $\rho_0 \sim T$), nine possible variants of the temperature dependence of ρ_0. Because m and p are interrelated, the following method of their determination is proposed. As follows from equation (1), in the temperature interval where T_{0j} is constant the local activation energy, $E_a(T) = \mathrm{d}\ln\rho(T)/\mathrm{d}(kT)^{-1}$ [12], can be presented in the form

$$\ln[E_a/(kT) + m] = \ln p + p\ln T_{0j} + p\ln(1/T). \tag{6}$$

In an ideal case the left-hand side of equation (6) represents a linear function of $\ln(1/T)$ for a single value of m. Then p can be found from the slope of this plot. In practice, one should analyse this dependence in a limited temperature interval above T_m. Therefore, the plots of $\ln[E_a/(kT)+m]$ versus $\ln(1/T)$ would be linear functions within some error for various m. In this situation it is more consistent to vary m within some interval and to determine p for each value of m, which gives the function of $p(m)$. Using this function, one can choose a proper pair of m and p in agreement with those in table 2.

As shown in figures 3 and 4, the plot of $p(m)$ for each sample gives a single pair (p, m) out of the possible combinations shown in table 2. For all samples the value of $p \approx 0.5$, corresponding to the existence of the soft Coulomb gap, is found. In no 3-3 the slightly lower $p \approx 0.48$ is due to a larger error in the relatively narrow interval of the linear dependence (see the inset to figure 3). On the other hand, $m \approx 4.5$ for no 3-0 is decreased to $m \approx 2.5$ for no 3-3, 3-7 and 3-9. For $\Gamma \gg 1$ this corresponds to a change of the form of the wavefunction of the localized carrier as described in the appendix. Hence, doping with Fe influences strongly the electronic properties of LCMO by inducing additional microscopic structural disorder in the cation sublattice of LCMO. In the insets to figures 3 and 4 are shown the dependencies of $\ln[E_a/(kT) + m]$ on $\ln(1/T)$ for $m = 5/2$ and $9/2$, giving the temperature of the onset of the SE-VRH regime (see table 1).

In figure 5 are displayed the dependencies of $\ln(\rho/T^m)$ versus $T^{-1/2}$ (curves 1) for no 3-0 ($m = 9/2$) and no 3-3, 3-7 and 3-9 ($m = 5/2$). They are compared with the plots of $\ln(\rho/T)$ versus T^{-1} corresponding to the NNH regime (curves 2). The curves are fitted with linear functions (dotted lines). The scales are picked up so that both lines have the same initial

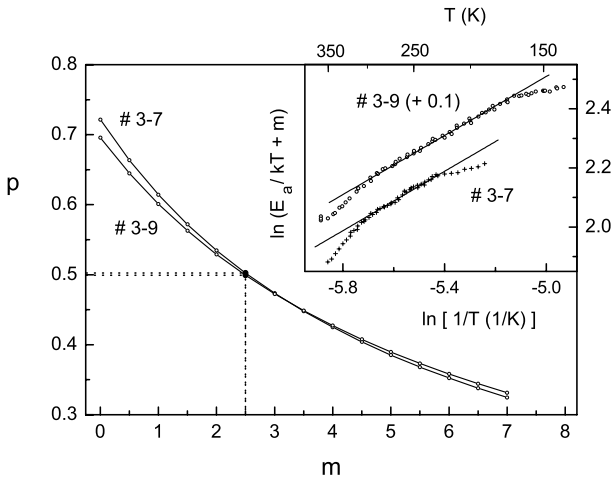

Figure 4. Dependence of p on m for no 3-7 and no 3-9. Inset: dependence of $\ln(E_a/kT+m)$ on $\ln(1/T)$ for $m = 5/2$. The lines are fits to the experimental data.

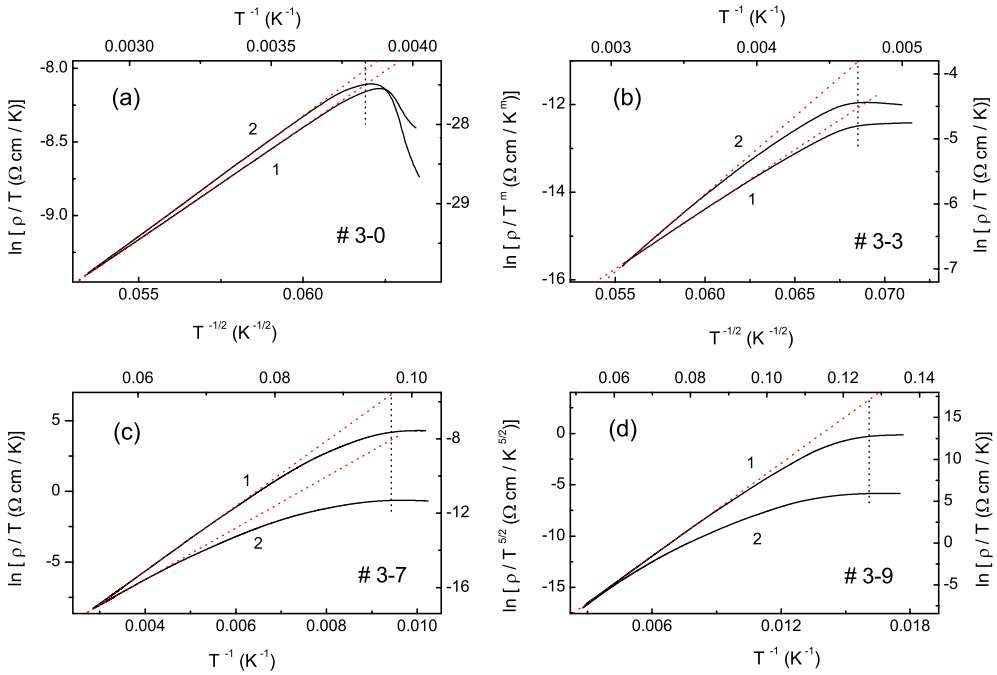

Figure 5. Comparison of the plots of $\ln(\rho/T^m)$ versus $T^{-1/2}$ ($m = 9/2$ for no 3-0 and $5/2$ for no 3-3, 3-7 and 3-9) (curves 1) and $\ln \rho/T$ versus T^{-1} (curves 2) for (a) no 3-0, (b) no 3-3, (c) no 3-7 and (d) no 3-9. The dotted lines are linear fits and the vertical dotted lines correspond to T_m for both temperature axes.

point and T_m^{-1} and $T_m^{-1/2}$ lie at opposite points of the T^{-1} and $T^{-1/2}$ axes (they are given by the vertical dotted lines). Neither of the plots contains a linear part up to T_m. Hence, the quality of the linear fitting for each curve is given by an area of the figure lying between the curve, the fitting line and the vertical dotted line corresponding to T_m. As can be seen from

figure 5(a), although the linear parts of lines 1 and 2 for no 3-0 are almost the same, the area of the corresponding figure constructed for line 1 is measurably smaller than that of line 2. For samples no 3-3, 3-7 and 3-9 the difference between these figures is much larger. Therefore, the SE VRH conductivity model describes the resistivity much better than the NNH model, in agreement with the conclusion drawn from figures 3 and 4.

The linear part of the plots $\ln(\rho/T^m)$ versus $T^{-1/2}$ in figure 5 yields T_0 and A collected in table 1. The values of Δ evaluated with equation (A.14) are quite close to the interval of the parabolic dependence of DOS ($\sim$0.4 eV) found experimentally in [13]. The existence of the temperature interval where T_0 is constant, as is evident from figures 3–5, suggests that one of the cases, mentioned in comments to equation (5), takes place. To find which case is realized, we analyse the temperature dependence of the resistivity in the magnetic field. The localization radius of small polarons in the PM phase was predicted to vary in the field according to the law [22]

$$a(B) = a(0)(1 + b_1 B^2), \tag{7}$$

where $b_1 \sim \chi(T)$. If $b_1 B^2 \ll 1$, it follows from equations (2), (5) and (7) that

$$T_0(B) = T_0(0)(1 - b_2 B^2), \tag{8}$$

where $b_2 = b_1 T_{0SE}(0)\{T_0(0) - [T_0(0)/T]^{1/2}\delta/(2k)\}^{-1}$ until δ is independent of the magnetic field. This gives

$$\delta(T) = 2\frac{b_1/b_2 - 1}{2b_1/b_2 - 1} k\sqrt{T_0(0)T}. \tag{9}$$

Near T_v, which is well above T_C, the temperature dependence of χ can be neglected (see figure 1). Therefore, in the temperature intervals in the vicinity of T_v the dependencies of T_0 and A on B for no 3-3, 3-7 and 3-9 can be found from linear fits of the plots of $\ln(\rho/T^{5/2})$ versus $T^{-1/2}$ in the field. For no 3-0 these dependencies could not be obtained because the interval of the linearity of the plots of $\ln(\rho/T^{9/2})$ versus $T^{-1/2}$ in the field was found to be insufficient. The dependence of $a(B)/a(0)$ can be evaluated with equation (A.12). As can be seen from figure 6 the plots of $a(B)/a(0)$ versus B^2 are linear functions up to $B = 10$ T, while those of $T_0(B)/T_0(0)$ versus B^2 are linear up to $B \approx 8$ T. As is evident from table 1, the values of the ratio of b_1/b_2 are found to lie above unity and the deviation from unity is much larger than the error. This means the existence of a non-zero rigid gap near T_v with values of $\delta(T_v)$ shown in table 1.

To estimate the localization radius, we use the density of states proposed by Viret *et al* [8], $g_0 \approx N_0 \phi g \eta / W$, where $N_0 = 1.74 \times 10^{22}$ cm^{-3} is the concentration of Mn sites, W is the width of the band of the localized states, $\eta \approx c = x - y$ is the concentration of the holes or the probability that the Mn site receiving the hopping electron is unoccupied, $\phi \approx 0.5$ is a geometric factor and $g \approx 1 - c$ is the probability that an unoccupied Mn site can actually accept an electron. The values of W can be calculated using the equation $kT_C \approx 0.05Wc(1 - c)$ predicted by Varma [22]. Then κ was evaluated with equation (A.13) and finally a was found using equations (2) and (5) (see table 1). The obtained value of $\kappa \approx 3.4$ is smaller than the static dielectric constant, $\kappa_0 = 16$ [23], because the average distance between the holes in LCMFO, $R = 2(4\pi c N_0/3)^{-1/3}$, is about the lattice parameter $l \approx 7.7$ Å of the cubic LCMO structure [18]. This does not permit the performance of macroscopic averaging of the Coulomb interactions of the holes, so that κ does not represent a true dielectric constant, but rather an effective parameter lying between the limits 1 and κ_0, corresponding to interactions in a vacuum and in a medium. The values of a are smaller than the average distance between the Mn sites, $R_0 = 2(4\pi N_0/3)^{-1/3} = 4.8$ Å, satisfying the requirement for small polaron formation [11]. It can be shown also that the condition of $\Gamma \gg 1$ is satisfied.

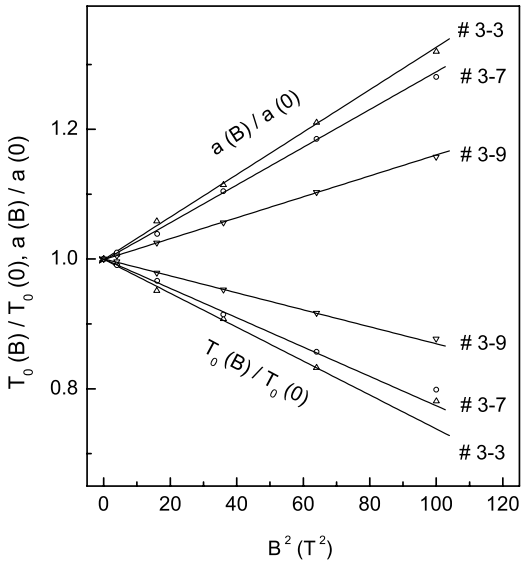

Figure 6. The dependencies of $T_0(B)/T_0(0)$ and $a(B)/a(0)$ on B^2. The full lines are linear fits.

As follows from the analysis above, in the temperature interval where T_0 is constant the dependence of δ on T should be close to $\sim T^{1/2}$ (see comments to equation (5)). It is possible to evaluate the function $\delta(T)$ within a wider temperature interval, using the magnetic field dependence of T_0 and the localization radius a shown in figure 6. Below, the values of the parameters inside the interval where T_0 is constant are marked by an asterisk (i.e. a^*, T_0^* and T_{0SE}^*). Then, from equations (1), (4) and (A.12), excluding the unknown constant C, we obtain the first equation

$$\ln\left[\frac{\rho(T)}{\rho(T_v)}\left(\frac{T_v}{T}\right)^{5/2}\right] = 11\ln\left(\frac{a}{a^*}\right) + \frac{11}{2}\ln\left(\frac{T_0}{T_0^*}\right) + \left(\frac{T_0}{T}\right)^{1/2} - \left(\frac{T_0^*}{T_v}\right)^{1/2} \quad (10)$$

connecting T_0 and a. The second equation can be written in the form

$$T_0/T_0^* = f(a/a^*) \quad (11)$$

where the function $f(\gamma)$ can be obtained by excluding B from the magnetic field dependencies of $T_0(B)/T_0(0)$ and $a(B)/a(0)$ in figure 6 (this gives a weakly nonlinear function which can be approximated with a second-order polynomial). The solutions of the pair of equations (10) and (11) within the intervals of $1 \leqslant a/a^* \leqslant [a(B)/a(0)]_{max}$ and $[T_0(B)/T_0(0)]_{min} \leqslant T_0/T_0^* \leqslant 1$, for no 3-7 are shown in figure 7 (for the other samples they are similar). Using the second of equations (2), we obtain the relative variation of $T_{0SE}/T_{0SE}^* = a^*/a$. On the other hand, from equation (5) taken at $T = T_v$ and the data in table 1 we find $T_{0SE}^* = T_0^* - (T_0^*/T_v)^{1/2}\delta(T_v)/k$, for the temperature dependence of the absolute value of T_{0SE}. Finally, using the temperature dependencies of T_0 and T_{0SE} the function $\delta(T)$ can be evaluated with equation (5). The result is shown in figure 8 along with the function $\delta(T_v)(T/T_v)^{1/2}$ (full lines).

As can be seen from figure 7, for no 3-7 at $B = 0$ a is constant at temperatures well above $T_C \approx 150$ K (see figure 1) and increases when $T \to T_C$. In a magnetic field the dependence of a on T becomes stronger and the interval of constancy of a is decreased. Trying to evaluate $a(T)$, $T_0(T)$ and $T_{0SE}(T)$ beyond the intervals of $1 \leqslant a/a^* \leqslant [a(B)/a(0)]_{max}$ and $[T_0(B)/T_0(0)]_{min} \leqslant T_0/T_0^* \leqslant 1$, at which $f(\gamma)$ was determined from the magnetic field

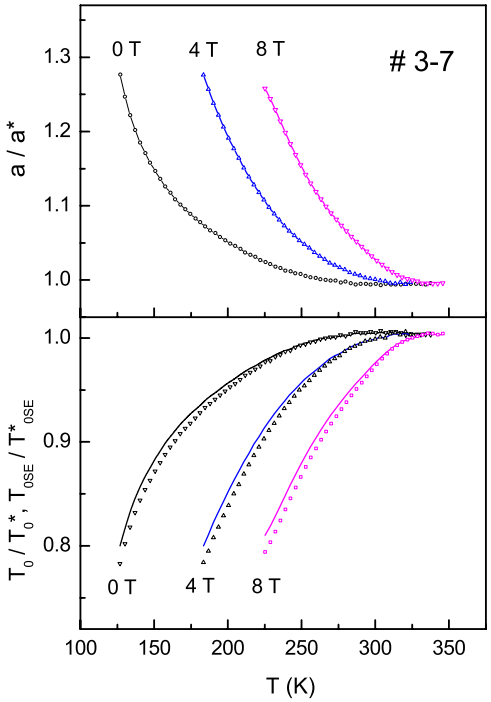

Figure 7. Temperature dependence of a/a^* in the fields 0, 4 and 8 T (upper panel) and of T_0/T_0^* (full curves) and T_{0SE}/T_{0SE}^* (symbols) (lower panel).

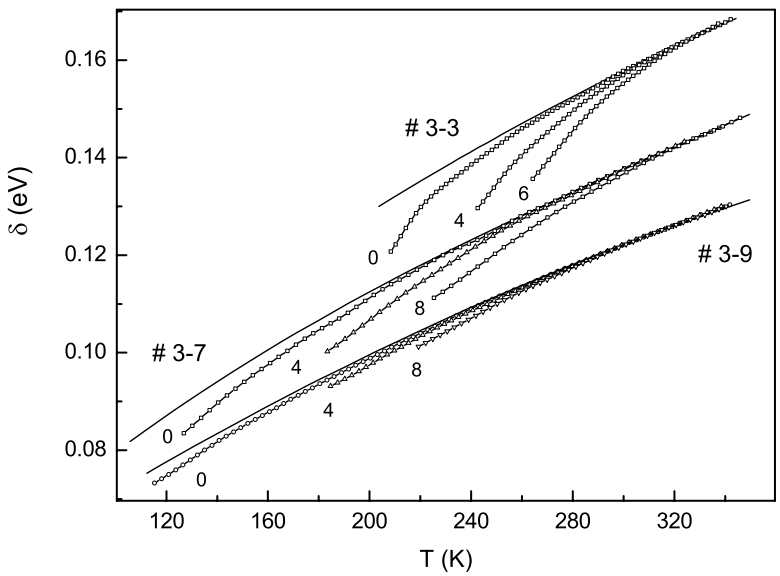

Figure 8. Temperature dependence of δ (lines with symbols) and $\delta(T_v)(T/T_v)^{1/2}$ (full lines) for no 3-3, 3-7 and 3-9 in zero field or in the fields of 4, 6 or 8 T. Near each curve is given the value of the field B in T.

dependencies in figure 6, we found that these parameters are finite down to T_m, below which the system of equations (10) and (11) has no solutions. On the other hand, the conventional metal–insulator transition requires a divergence of a which is not observed down to T_m.

As follows from figure 8, at temperatures well above T_C, δ is close to $\delta(T_v)(T/T_v)^{1/2}$ but deviates from it as $T \to T_C$. The deviation increases with increasing magnetic field and decreases when y is increased. The absolute value of δ decays with y, as well. In our LCMFO samples the values of $\delta(T_C)$ are similar to $\delta = 0.11$ eV in LCMO with $x = 0.2$ [13]. Those of $\delta(T_v)$ are close to the polaron binding energy, $W_p \approx 2W_h \approx 0.15$ eV, in LCMO found from the data of $\rho(T)$ between 300 and 700 K [5].

4. Conclusions

Resistivity of $La_{0.7}Ca_{0.3}Mn_{1-y}Fe_yO_3$ with $y = 0.0$, 0.03, 0.07 and 0.09 is investigated at temperatures between 4.2 and 350 K and in magnetic fields between $B = 0$ and 10 T. It is shown that the charge transfer above the PM–FM transition is governed by the Shklovskii–Efros-type VRH conductivity mechanism, determined by the existence of a soft parabolic Coulomb gap and, additionally, by a rigid gap in the spectrum of the density of localized states around the Fermi level. The rigid gap depends on temperature. Well above T_C this dependence is close to $\delta(T) \sim T^{1/2}$ but, as T approaches T_C, $\delta(T)$ exhibits deviations from the square root behaviour. In addition, it decreases when the concentration of Fe is increased. Near the temperature of the onset of VRH conductivity the values of δ are close to the polaron binding energy, while at $T \sim T_C$ they are similar to the value found by scanning–tunnelling spectroscopy measurements in [13]. The prefactor of the resistivity follows the temperature dependence $\rho_0 \sim T^m$, where m changes from 9/2 at $y = 0$ to 5/2 at $y = 0.03$, 0.07 and 0.09. This corresponds to transformation of the wavefunction of the localized charge carriers from a conventional hydrogen-like form $\psi(r) \sim \exp(-r/a)$ to $\psi(r) \sim r^{-1}\exp(-r/a)$, giving evidence that doping with Fe increases the microscopic disorder by introducing an additional fluctuating short-range potential.

Acknowledgments

This work was supported by the Wihuri Foundation, Finland, and by INTAS (project No INTAS 00-00728).

Appendix. Prefactor ρ_0 and the characteristic temperature T_0 of VRH conductivity

Shklovskii and Efros [12] have considered the hopping conductivity as a problem of percolation over the Miller–Abrahams random resistivity network [21]. A transition from the site i with the energy level $\varepsilon_i < \mu$ to the site j with $\varepsilon_j > \mu$ is associated with a resistivity $R_{ij} = R^0_{ij}\exp(\xi_{ij})$ between these sites, where

$$\xi_{ij} = \frac{2r_{ij}}{a} + \frac{\varepsilon_{ij}}{kT}, \tag{A.1}$$

$\varepsilon_{ij} = \varepsilon_j - \varepsilon_i$, r_{ij} is the distance between the sites and R^0_{ij} is a prefactor. The onset of percolation over the network corresponds to the percolation threshold ξ_c, which, for the Mott and SE VRH mechanisms (at $\delta = 0$), are given by the expressions $\xi_c = (T_{0M}/T)^{1/4}$ and $\xi_c = (T_{0SE}/T)^{1/2}$, respectively. Generally, ξ_c can be found from the bonding condition

$$\xi_{ij} \leqslant \xi \tag{A.2}$$

where ξ is the bonding parameter. Then the net specific resistivity can be written as

$$\rho(T) = \rho_0(T) \exp \xi_c, \tag{A.3}$$

where

$$\rho_0(T) = L_0 R^0_{ij} | \xi_{ij} = \xi_c. \tag{A.4}$$

Here $L_0 = r_0 \xi_c^{\nu}$ is the correlation radius of the critical subnet or the infinite cluster, corresponding to $\xi = \xi_c + 1$, $\nu \approx 1$ is the critical exponent of the correlation length, $r_0 = \sigma a \xi_c$ is the mean distance between the sites with energies inside the Mott optimum stripe, $\sigma \approx 2p(1-p)$, $R^0_{ij} = kT/(e^2 \gamma^0_{ij})$ and γ^0_{ij} is the prefactor of the hopping frequency given by

$$\gamma^0_{ij} = \frac{E_1^2 \varepsilon_{ij}}{\pi d s^5 \hbar^4} \left(\frac{2e^2}{3\kappa a} \right)^2 \frac{r_{ij}^2}{a^2} \left[1 + \left(\frac{\varepsilon_{ij} a}{2\hbar s} \right)^2 \right]^{-4} \left(\frac{a}{r_{ij}} \right)^q. \tag{A.5}$$

In equation (A.5) E_1 is the deformation potential constant, d is the material density, $q = 0$ for a localized state with the conventional hydrogen-like wavefunction $\psi(r) \sim \exp(-r/a)$ and $q = 4$ in the presence of microscopic structural defects providing a fluctuating short-range potential changing $\psi(r)$ to $\psi(r) \sim r^{-1} \exp(-r/a)$ [12].

The maximum energy and distance compatible with equation (A.2) are

$$\varepsilon_{max}(\xi) = kT\xi \qquad \text{and} \qquad r_{max}(\xi) = a\xi/2. \tag{A.6}$$

The concentration of the sites inside the interval $\mu - \varepsilon_{max}(\xi) < \varepsilon < \mu + \varepsilon_{max}(\xi)$ can be found by integration of the DOS (see figure 2) as $N(\xi) = 2\alpha_3 \kappa^3 (kT\xi - \delta)^3/(3e^6)$ and the total number of the sites as $n(\xi) = 4\pi r^3_{max} N/3 = (\pi \alpha_3/9)(\kappa^3/e^6)(kT)^3[\xi - \delta/(kT)]^3 \xi^3$. The percolation threshold satisfies the equation $n(\xi_c) = n_c$, where n_c is the critical value of the onset of the percolation. Then, taking into account the relation $\beta_{SE} = [9n_c/(\pi\alpha_3)]^{1/3}$ and the second of equations (2), ξ_c can be presented in a form similar to those of the Mott and SE VRH models:

$$\xi_c = \left(\frac{T_0}{T} \right)^{1/2}, \tag{A.7}$$

where

$$T_0 = \left(\frac{\delta}{2k\sqrt{T}} + \sqrt{\frac{\delta^2}{4k^2 T} + T_{0SE}} \right)^2. \tag{A.8}$$

Substituting $\varepsilon_{ij} = \varepsilon_{max}(\xi_c)$ and $r_{ij} = r_{max}(\xi_c)$ in equation (A.5), we get

$$\gamma^0_{ij}|_{\xi_{ij}=\xi_c} = \frac{E_1^2 kT \xi_c}{\pi d s^5 \hbar^4} \left(\frac{2e^2}{3\kappa a} \right)^2 \frac{\xi_c^2}{4} \left[1 + \left(\frac{kT\xi_c a}{2\hbar s} \right)^2 \right]^{-4} \left(\frac{2}{\xi_c} \right)^q, \tag{A.9}$$

where the second term inside the square brackets is equal to Γ defined by equation (3).

Using equations (A.4) and (A.9) $\rho_0(T)$ can be presented in the form

$$\rho_0 = C_0 a^3 (T_{0j}/T)^{(q-1)p} (1 + \Gamma)^4, \tag{A.10}$$

where $C_0 = 9\pi\sigma d s^5 \kappa^2 \hbar^4/(2^q E_1^2 e^6)$. In the limiting cases of $\Gamma \ll 1$ and $\Gamma \gg 1$, $\rho_0(T)$ is given by the equation

$$\rho_0(T) = AT^m, \tag{A.11}$$

where for $\Gamma \ll 1$ the expression for A is evident and for $\Gamma \gg 1$ it can be written as

$$A = (C/2^q) a^{11} T_{0j}^{(7+q)p} \tag{A.12}$$

with $C = 9\pi\sigma d \kappa^2 k^8/(256 E_1^2 e^6 s^3 \hbar^4)$. The values of m are collected in table 2.

Finally, putting $g(\mu \pm \Delta) = g_0$ and $\varepsilon_{max}[\xi_c(T_v)] = \Delta$, where T_v is the temperature of the onset of VRH conductivity, we obtain the following useful relations:

$$g_0 = \alpha_3(\kappa^3/e^6)(\Delta - \delta)^2 \tag{A.13}$$

and

$$\Delta = k(T_0T_v)^{1/2}. \tag{A.14}$$

References

[1] Von Helmolt R, Wecker J, Holzapfel B, Schulz L and Sammer K 1993 *Phys. Rev. Lett.* **71** 2331
[2] Schiffer P, Ramirez A P, Bao W and Cheong S-W 1995 *Phys. Rev. Lett.* **75** 3336
[3] Millis A J, Littlewood P B and Shairman B I 1995 *Phys. Rev. Lett.* **74** 5144
[4] Ramirez A P 1997 *J. Phys.: Condens. Matter* **9** 8171
[5] Snyder G J, Hiskes R, DiCarolis S, Beasley M R and Geballe T H 1996 *Phys. Rev.* B **53** 14 434
[6] Jaime M, Salamon M B, Rubinstein M, Treece R E, Horwitz J S and Chrisei D B 1996 *Phys. Rev.* B **54** 11 914
[7] Palstra T T, Ramirez A P, Cheong S-W, Zegarski B R, Schiffer P and Zaanen J 1997 *Phys. Rev.* B **56** 5104
[8] Viret M, Ranno L and Coey J M D 1997 *Phys. Rev.* B **55** 8067
[9] Hasanain S K, Nadeem M, Shah W H, Akhtar M J and Hasan M M 2000 *J. Phys.: Condens. Matter* **12** 9007
[10] Sun Y, Xu X and Zhang Y 2000 *J. Phys.: Condens. Matter* **12** 10 475
[11] Mott N F and Davies E A 1979 *Electron Processes in Non-Crystalline Materials* (Oxford: Clarendon)
Mott N F 1990 *Metal–Insulator Transitions* (London: Taylor and Francis)
[12] Shklovskii B I and Efros A L 1984 *Electronic Properties of Doped Semiconductors* (Berlin: Springer)
[13] Biswas A, Elizabeth S, Raychaudhuri A K and Bhat H L 1999 *Phys. Rev.* B **59** 5368
[14] Ahn K H, Wu X W, Liu K and Chien C L 1996 *Phys. Rev.* B **54** 15 299
[15] Jonker G H 1954 *Physica* **20** 1118
[16] Simopoulos A, Pissas M, Kallias G, Devlin E, Moutis N, Panagiotopoulos I, Niarchos D, Christides C and Sonntag R 1999 *Phys. Rev.* B **59** 1263
[17] Laiho R, Lisunov K G, Lähderanta E, Salminen J and Zakhvalinskii V S 2002 *J. Magn. Magn. Mater.* at press
[18] Laiho R, Lisunov K G, Lähderanta E, Petrenko P, Stamov V N and Zakhvalinskii V S 2000 *J. Magn. Magn. Mater.* **213** 271
[19] Castner T G 1991 *Hopping Transport in Solids* ed M Pollak and B Shklovskii (Amsterdam: Elsevier) p 3
[20] Zheng R K, Zhu C F, Xie J Q and Li X G 2000 *Phys. Rev.* B **63** 024427
[21] Miller A and Abrahams E 1960 *Phys. Rev.* **120** 745
[22] Varma C M 1996 *Phys. Rev.* B **54** 7328
[23] Alexandrov A S and Bratkovsky A M 2000 *J. Appl. Phys.* **87** 5016